Articles

Characterization of COK-5, Member of a New Family of Zeolite Material with Multiple Channel Systems

Christine Kirschhock,[†] Anton-Jan Bons,[‡] Machteld Mertens,[‡] Raman Ravishankar,[†] Wilfried Mortier,[‡] Pierre Jacobs,[†] and Johan Martens*,[†]

Center for Surface Chemistry and Catalysis, Catholic University of Leuven, Kasteelpark Arenberg 23, B-3001 Leuven, Belgium, and ExxonMobil Chemical Europe Inc., European Technology Center, Hermeslaan 2, B-1831 Machelen, Belgium

Received January 31, 2005. Revised Manuscript Received June 22, 2005

In this paper we propose a structure for the novel zeolite material COK-5. COK-5 has a distinct X-ray diffraction pattern, showing unique peaks and broad features. This suggests a layered structure with stacking disorder, consistent with SEM and TEM observations. The proposed structure builds on modified structure elements of MFS type zeolite. The building layers can be stacked in various ways, leading to three new structures, termed Mirror, Glide, and Centre. We propose COK-5 is an intergrowth of these new structures and MFS. The COK-5 channel system comprises four types of pores with windows circumscribed with 10- or 12-rings of oxygen atoms. The refined constraint index of 2.7 situates COK-5 at the transition between 10-ring and 12-ring zeolites. The presence of four pore systems in the same material is unusual and promises high catalytic potential of COK-5.

Introduction

Zeolite materials frequently occur as intergrowths of two or more structures into another.[1,2] The inclusions and alternative stacking patterns often extend over very limited distances only. The intergrowths of the pentasil zeolite family,[3] the FAU−EMT intergrowths,[4,5] and the combinations of zeolite Beta polymorphs[6,7] are illustrative examples. There are instances where disorder does not block the pores nor alters the local pore topology, such as in SSZ-31,[8] and in ZSM-48 type zeolites.[9] In other instances, intergrowth formation can be a tool for altering the pore architecture and the cation-siting sought after in molecular shape selective catalysis and adsorption. Examples are small-pore versus large-pore variants of mordenite,[10] and ERI−OFF intergrowths.[11] Recently, we discovered a novel zeolite we named COK-5.[12] COK-5 is a highly faulted structure related to MFS with unique catalytic properties.

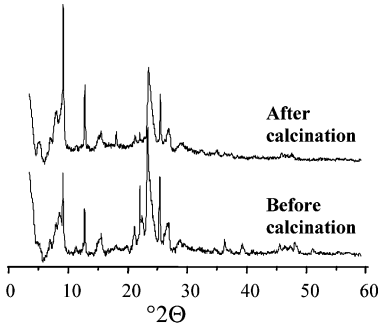

Figure 1. Powder XRD patterns of COK-5.

Table 1. Characteristics of the Powder X-ray Diffraction Pattern of COK-5

°2θ (Cu Kα radiation)	intensity	nature
6 to 8.7	weak/medium	broad feature
8.82 ± 0.1	strong	sharp
12.44 ± 0.5	medium	sharp
14 to 16	medium	broad feature
20.4 to 21.2	weak	broad feature
23.01 ± 0.1	very strong	sharp
22.5 to 24.5	medium/strong	broad feature
25.02 ± 0.1	variable, may be absent	sharp
25.5 to 27	medium	broad feature

* To whom correspondence should be addressed. Fax: +32 16 32 19 98. Tel: +32 16 32 1610. E-mail: johan.martens@agr.kuleuven.ac.be.
† Catholic University of Leuven
‡ ExxonMobil Chemical Europe Inc.

(1) Gies, H.; van Koningsveld, H. "Catalog of Disorder in Zeolite Frameworks" http://www.iza-structure.org/databases/.
(2) Dorset, D. L. *Z. Kristallogr.* **2003**, *218*, 458.
(3) Kokotailo, G. T.; Chu, P.; Lawton, S. L.; Meier, W. M. *Nature* **1978**, *275*, 119.
(4) Newsam, J. M.; Treacy, M. M. J.; Vaughan, D. E. W.; Strohmaier, K. G.; Mortier, W. J. *Chem. Commun.* **1989**, 493−495.
(5) Martens, J. A.; Van Butsele, G. M.; Jacobs, P. A. *Proceedings 9th International Zeolite Conference*; von Ballmoos, R., et al., Eds.; Butterworth-Heinemann: Woburn, MA, 1993; p 355.
(6) Newsam, J. M.; Treacy, M. M. J.; Koetsier, W. T.; de Gruyter, C. B. *Proc. R. Soc. London A* **1988**, *420*, 375−405.
(7) Corma, A.; Navarro, M. T.; Rey, F.; Valencia, S. *Chem. Commun.* **2001**, 1720−1721.
(8) van Koningsveld, H.; Lobo, R. F. *J. Phys. Chem. B* **2003**, *107*, 10983−10989.
(9) Lobo, R. F.; van Koningsveld, H. *J. Am. Chem. Soc.* **2002**, *124*, 13222−13230.
(10) Rudolf, P. R.; Garcés, J. M. *Zeolites* **1994**, *14*, 137−145.
(11) Martens, J. A.; Wydoodt, M.; Espeel, P.; Jacobs, P. A. *Stud. Surf. Sci. Catal.* **1993**, *78*, 527. Mortier, W. J.; Pluth, J. J.; Smith, J. V. Z. *Kristallografiya*. **1976**, *143*, 319.

10.1021/cm050227z CCC: $30.25
Published on Web 10/14/2005

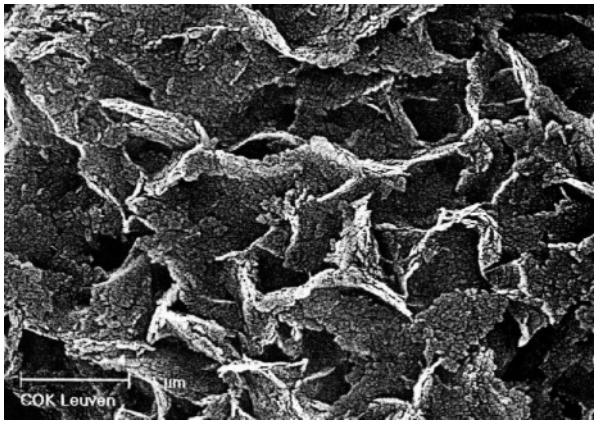

Figure 2. SEM micrograph of uncalcined COK-5.

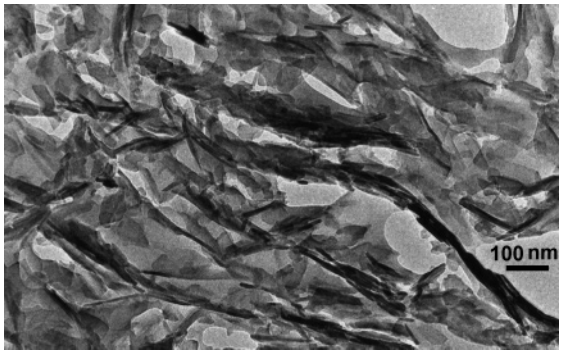

Figure 3. Low-magnification TEM micrograph showing the flaky nature of COK-5.

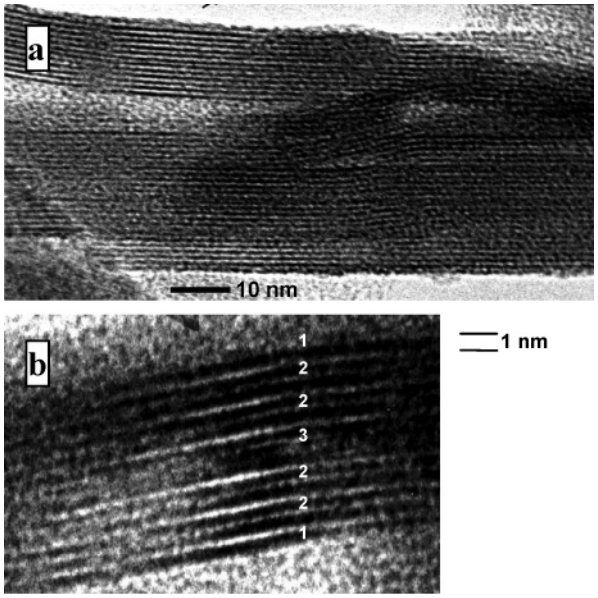

Figure 4. TEM lattice fringe images of COK-5, a: curved layers and layer splitting; b: a crystal with a 1-2-2-3-2-2-1 stacking sequence.

Experimental Section

Synthesis of COK-5. COK-5 was made according to example 1 of the original patent[12] and involves the use of *N*,*N*,*N*,*N*′,*N*′,*N*′-hexaethylpentane diammonium bromide (HEPDD) as template. Twenty-two grams of Ludox AS40, 1.5 g of sodium hydroxide (99%), and 26 g of water were mixed for 15 min. To this mixture

(12) Mertens, M. M.; Ravishankar, R.; Martens, J. A.; Kirschhock, C. E. A.; Jacobs, P. A.; Bons, A. J.; Mortier, W. J. Patent application: WO0246099A1, 2002.

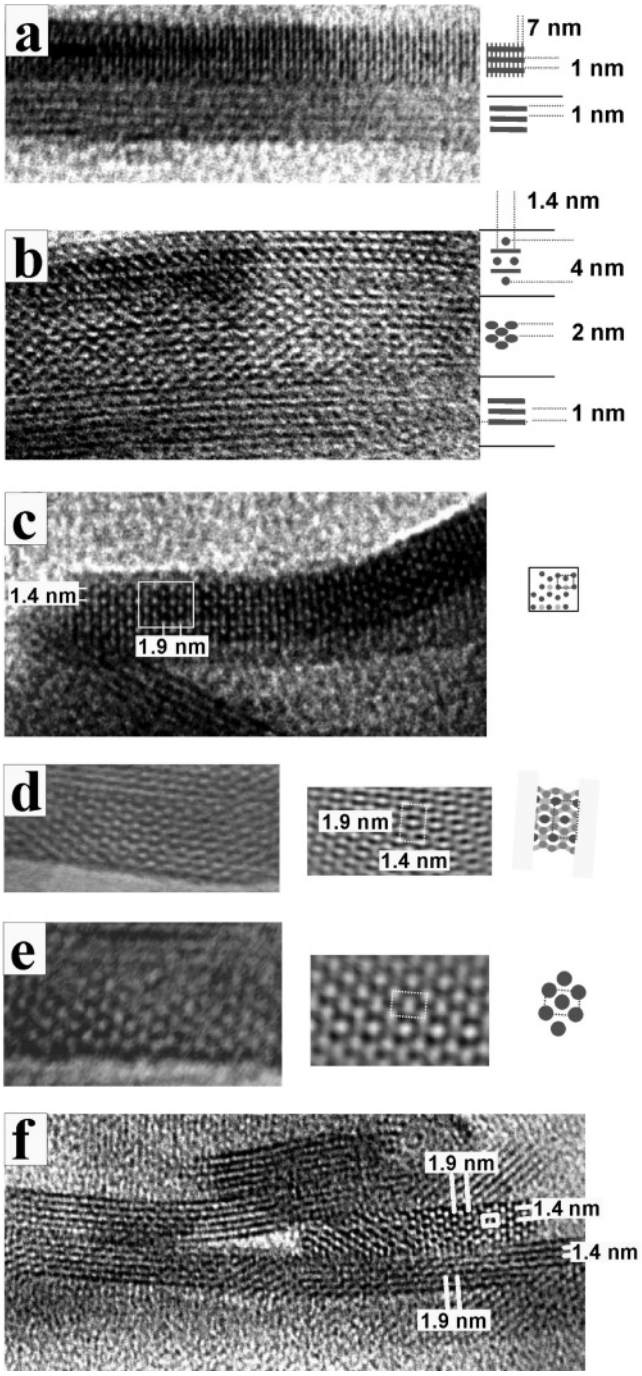

Figure 5. High-resolution TEM images of COK-5 crystals, showing layers with various image structure. A schematic of the image structure, or "imaging code", is given next to the layers. In many cases a 1.4 × 1.9 cell can be recognized. In (d) and (e) Fourier filtered images are placed next to the direct image.

Table 2. Refined Constrained Index of COK-5 and Several Other Zeolites

zeolite	code	refined constraint index	ethyl octane index	dimensionality index
BETA	BEA	1.4	7.1	1
USY	FAU	1.5	12.6	0
mordenite	MOR	1.8	6.5	33
ZSM-12	MTW	2.4	6	13
COK-5		**2.7**	**2.5**	**17.9**
ZSM-57	MFS	3.0	1.7	15.2
MCM-22	MWW	4.6	0.7	12
ZSM-35	FER	10.3	0	13
ZSM-22	TON	14.5	0	19

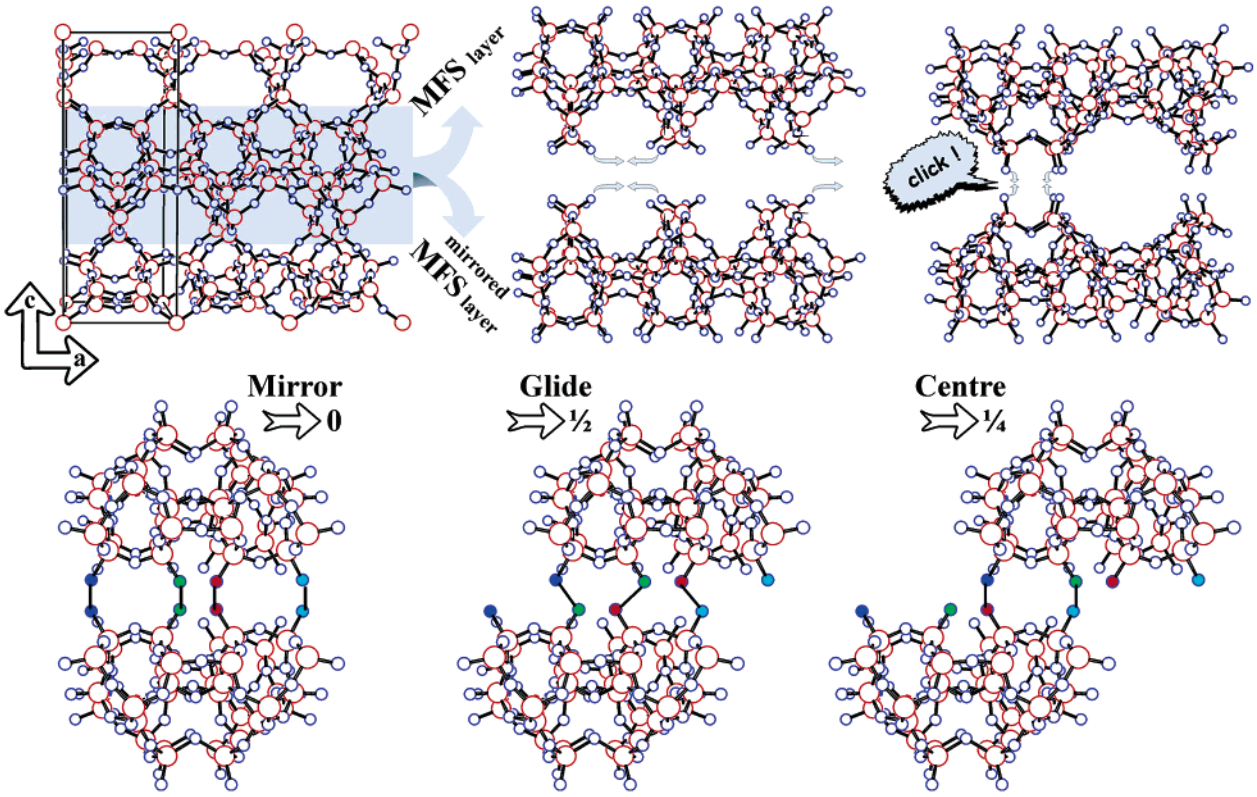

Figure 6. Three possible ways to connect a MFS layer to its mirror MFS′ layer.

was added a solution containing 0.42 g of sodium aluminate (Riedel-De Haen: 54% Al_2O_3; 41% Na_2O; 4.98% H_2O) and 26 g of water. The mixture was stirred for 10 min and a solution of 5.9 g of HEPDD in 36 g of water was added slowly and mixed for another 15 min. The mixture had the following molar composition:

$$66SiO_2:Al_2O_3:9.8Na_2O:6.17HEPDD:2541H_2O$$

The synthesis mixture was poured into a stainless steel autoclave and heated for 10 days at 150 °C. The solid product was recovered from the reaction mixture, washed, and dried at 60 °C for 3 h.

After calcination BET analysis shows a surface area of 345 m^2/g and a micropore volume of 0.11 mL/g.

Characterization of COK-5. SEM micrographs of COK-5 (Figure 1) appear homogeneous, showing thin flakes of roughly 1 μm wide and only a few tens of nanometers thick. The flakes are often curved and split out from each other.

The X-ray diffraction pattern of COK-5 is characterized by a few sharp Bragg reflections and broad features (Table 1, Figure 2). This combination suggests a faulted structure.[13]

The pore architecture of COK-5 was characterized using the decane hydroconversion test[14,15] (Table 2). In this catalytic test information on the pores is gained from the formation of specific reaction products. The Refined Constraint Index,[14] derived from the selectivity of 2- versus 5-methylnonane formation in decane hydro-isomerization, is 2.7, indicating a more open structure in COK-5 than in the 10-ring zeolite ZSM-57, but narrower than in the 12-ring zeolite ZSM-12.

The Ethyl Octane Index[14] based on the extent of formation of ethyloctane isomers having bulkier ethyl side chains leads to the same ranking of COK-5 among reference zeolites (Table 2). The high value of the dimensionality index[15] of 17.9 reflecting the occurrence of extensive secondary cracking suggests the presence of at least one monodimensional pore system.

Transmission electron microscopy (TEM) was done on a Philips CM12-T operated at 120 kV. Low-magnification TEM images confirm the flaky nature of COK-5 (Figure 3). The material appears to contain one single type of particles. It is beam-sensitive and allows little time for focusing or tilting the specimen. However, several flakes could be imaged edge-on. High-resolution TEM images show lattice fringes with spacings around 1 nm. The fringes are curved and split, comparable to clay minerals (Figure 4a). Sometimes grouping of fringes (Figure 4b) is observed.

At higher resolution the COK-5 crystals show a variety of image structures. The flakes clearly exhibit a layered structure, and in most flakes several layers with different image structure are intergrown (see Figure 5). A cell of 0.7 or 1.4 by 1.9 nm can be distinguished repeatedly. Some images (Figure 5d,e) were Fourier-filtered to reduce the noise due to the necessary low-dose conditions.

Results

Structure Interpretation and Simulations. As the XRD patterns show some similarity to ZSM-57[16] (MFS topology) with a unit cell of 0.7 × 1.4 × 1.9 nm, it is highly probable that the structure of COK-5 is related to ZSM-57. The constraint and dimensionality indices support this assumption.

The MFS structure can be constructed from 0.7 nm layers in the a−b plane stacked in the *c*-direction (Figure 6a). TEM analysis proves that the new material has a layered structure with exactly this repeat distance. The choice cut of the MFS structure accounts for this observation, when applying a

(13) Treacy, M. M. J.; Newsam, J. M.; Deem, M. W. *Proc. R. Soc. London* **1991**, *A433*, 499−520.
(14) Jacobs, P. A.; Martens, J. A. *J. Pure Appl. Chem.* **1986**, *58*, 1329.
(15) Olken, M. M.; Garcés, J. M. *Proceedings 9th International Zeolite Conference*, Montreal; von Ballmoos, R., et al., Eds.; Butterworth-Heinemann: Boston, MA, 1992; Vol. II, p 559.
(16) Schlenker, J. L.; Higgins, J. B.; Valyocsik, E. W. *Zeolites* **1990**, *10*, 293−296.

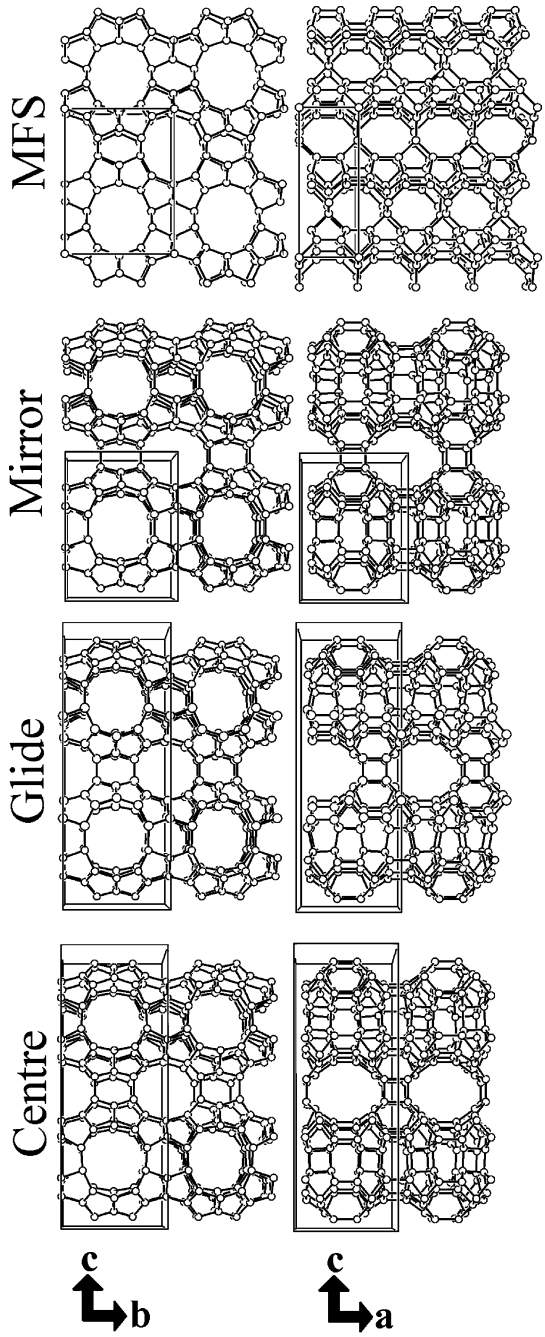

Figure 7. MFS and three new crystal structures derived from combining a MFS layer with its mirror MFS′ layer.

mirror operation rather than a translation of connecting layers. This forms sheets of parallel 10-ring tubes. On the other side the MFS layers have to be adapted to prevent edge-sharing SiO_4 tetrahedra. To evade this dilemma, opposing O−Si−O groups are condensed into O−Si−O−Si−O clusters (Figure 6). Neighboring layers are connected via the newly established click-contacts (Figure 6), forming rather open galleries. The formation of the click-contacts introduces a considerable strain in the structure. SEM and TEM images show direct evidence for stress in the layers. All flakes are curved, and the crystals do not extend sideways (=parallel to the layers) for a long distance; they always curve or split apart. Also the observation that stacking of identical layers does not extend further than a few layers, and the very thin plates, are indications of stress. A few layers can still accommodate small misfits by deforming, but after a few repeats the deformation is too large to fit another identical layer, and a different structure that fits better will grow, or growths stops altogether. These experimental indications of stress in the structure encourage further pursuit of the deduced structure model by describing it in crystallographic terms. Atomic coordinates, lattice symmetry, and unit cell constants are to be derived from the proposed model. Mapping the possible connectivities shows the tube sheets can be formed from two layers in three different ways by relative, lateral shifts along the tubes' direction. The three related structures are termed mirror (no translation), glide (a single or a triple translation in tube direction), and center (a double shift in tube direction, equivalent to a shift of half of the resulting unit cell constant). To obtain the atomic positions in the resulting tetrahedral frameworks, the structures were first refined with the General Utilisation Lattice Program (GULP) using the relax fitting option.[17] Compared to the MFS structure, the lattices are contracted in the former *a*-direction and stretched in the corresponding *c*-direction. This is an expected result of the formation of the click-contacts (Figure 6). Those coordinates were used in the program DLS-76[18] to verify the connection rules of rigid SiO_4 units are obeyed.

Table 3. Fractional Coordinates of Mirror as Refined by DLS-76 (*Pmmm*, $a = 13.98$ Å, $b = 14.46$ Å, $c = 19.09$ Å; Rvalue = 0.9%)

atom	x	y	z
Si1	0.261	0.000	0.232
Si2	0.278	0.202	0.198
Si3	0.389	0.317	0.081
Si4	0.387	0.000	0.351
Si5	0.355	0.188	0.425
Si6	0.396	0.307	0.307
Si7	0.297	0.500	0.132
Si8	0.387	0.500	0.281
Si9	0.112	0.000	0.361
Si10	0.138	0.202	0.425
Si11	0.107	0.299	0.276
Si12	0.110	0.500	0.225
O1	0.254	0.093	0.184
O2	0.369	0.000	0.266
O3	0.334	0.242	0.129
O4	0.347	0.221	0.265
O5	0.389	0.280	0.000
O6	0.323	0.409	0.085
O7	0.500	0.000	0.370
O8	0.337	0.093	0.382
O9	0.249	0.231	0.441
O10	0.419	0.267	0.385
O11	0.500	0.328	0.270
O12	0.500	0.500	0.300
O13	0.373	0.500	0.196
O14	0.338	0.405	0.311
O15	0.406	0.163	0.500
O16	0.500	0.333	0.105
O17	0.181	0.000	0.293
O18	0.179	0.253	0.218
O19	0.000	0.000	0.337
O20	0.134	0.092	0.407
O21	0.108	0.259	0.356
O22	0.000	0.282	0.244
O23	0.000	0.500	0.197
O24	0.188	0.500	0.161
O25	0.127	0.410	0.274
O26	0.084	0.221	0.500

(17) Gale, J. D.; Rohl, A. L. *Mol. Simul.* **2003**, *29*, 291.
(18) Baerlocher, C.; Hepp, A.; Meier, W. M. DLS-76: A distance least squares refinementprogram, ETH, Zurich, 1977.

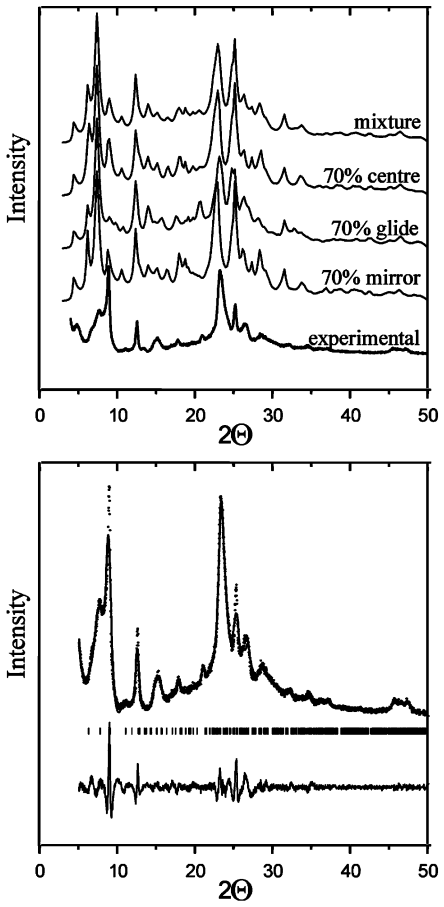

Figure 8. Simulation of experimental X-ray pattern. Top: Diffax simulations containing either predominantly one phase or a random mixture. Bottom: Rietveld refinement based on atomic coordinates of the Centre structure (Rp = 6.0%; Rwp = 8.5%).

As a result, three new crystal structures are proposed, all derived from the MFS layer (see Figure 7, Tables 3−5).[19] For Glide and Centre two crystallographic settings are given, the second allowing direct comparison with the MFS topology.

Mirror, DLS-76 reliability factor: 0.9%
Pmmm, $a = 13.98$ Å, $b = 14.46$ Å, $c = 19.09$ Å

Glide, DLS-76 reliability factor: 0.7%
*P*2/*m*, $a = 18.68$ Å, $b = 14.42$ Å, $c = 14.27$ Å, $\beta = 76.59$; 0.7%
'*P*2*mm*', $a' = 2*7.14$ Å, $b = 14.42$ Å, $c' = 2*18.17$ Å

Centre, DLS-76 reliability factor: 0.6%
Cmmm, $a = 14.39$ Å, $b = 37.67$ Å, $c = 14.47$ Å
'*Bmmm*', $a = 2*7.20$ Å, $b' = 14.47$ Å, $c' = 2*18.84$ Å

MFS, *Imm*2, $a = 7.45$ Å, $b = 14.17$ Å, $c = 18.77$ Å

Planar intergrowth can occur between any of the four structures

DIFFaX[13,19] simulations of intergrowths of these structures show features similar to the experimental pattern (Figure 8). However, the slight mismatch of lattice parameters in the stacking planes cannot be accounted for by DIFFAX simulations because no local relaxation of atomic coordinates is foreseen. For this reason a Rietveld refinement with the GSAS program package[20] was attempted. TEM study and DIFFAX simulation pointed to the dominant occurrence of the Centre structure intergrown with Glide domains and to a lesser degree Mirror layers. Rietveld refinement used the

Table 4. Fractional Coordinates of Glide as Refined by DLS-76 (*P*2/*m*, $a = 18.68$ Å, $b = 14.42$ Å, $c = 14.27$ Å, $\beta = 76.59$; Rvalue = 0.7%)

atom	x	y	z
Si1	0.284	0.000	0.220
Si2	0.371	0.000	−0.005
Si3	0.418	0.193	0.024
Si4	0.267	0.296	0.037
Si5	0.207	0.500	0.059
Si6	0.230	0.205	0.240
Si7	0.105	0.311	0.389
Si8	0.421	0.000	0.312
Si9	0.235	0.000	0.670
Si10	0.180	0.205	0.674
Si11	0.063	0.311	0.613
Si12	0.401	0.000	0.545
Si13	0.444	0.203	0.592
Si14	0.312	0.296	0.542
Si15	0.108	0.500	0.694
Si16	0.269	0.500	0.545
Si17	0.466	0.181	0.196
Si18	0.327	0.000	0.815
Si19	0.405	0.196	0.789
Si20	0.252	0.297	0.834
Si21	0.191	0.500	0.852
Si22	0.362	0.297	0.317
Si23	0.156	0.500	0.269
Si24	0.302	0.500	0.327
O1	0.232	0.908	0.236
O2	0.333	0.000	0.109
O3	0.338	0.000	0.294
O4	0.308	0.000	0.932
O5	0.419	0.906	-0.032
O6	0.402	0.168	0.138
O7	0.500	0.238	0.000
O8	0.352	0.262	0.008
O9	0.227	0.272	0.949
O10	0.224	0.246	0.136
O11	0.259	0.408	0.053
O12	0.167	0.500	0.969
O13	0.144	0.500	0.160
O14	0.307	0.243	0.262
O15	0.162	0.236	0.328
O16	1.021	0.282	0.386
O17	0.110	0.318	0.501
O18	0.122	0.409	0.331
O19	0.416	0.000	0.428
O20	0.467	0.909	0.265
O21	0.313	0.000	0.590
O22	0.188	0.093	0.659
O23	0.251	0.000	0.778
O24	0.206	0.238	0.771
O25	0.096	0.233	0.675
O26	0.229	0.258	0.580
O27	0.065	0.409	0.670
O28	0.440	0.091	0.578
O29	0.361	0.246	0.607
O30	0.500	0.249	0.500
O31	0.468	0.223	0.693
O32	0.344	0.267	0.430
O33	0.316	0.408	0.558
O34	0.119	0.500	0.805
O35	0.190	0.500	0.624

(19) Martens, J. A.; Ravishankar, R.; Mishin, I. E.; Jacobs, P. A. *Angew. Chem., Int. Ed.* **2000**, *39*, 4376

(20) Larson, A. C.; Von Dreele, R. B. *General Structure Analysis System (GSAS)*; Los Alamos National Laboratory Report LAUR 86-748; Los Alamos National Laboratory: Los Alamos, NM, 2000.

Table 5. Fractional Coordinates of Centre as Refined by DLS-76 and Used for Rietveld Refinement (*Cmmm*, $a = 14.39$ Å, $b = 37.67$ Å, $c = 14.47$ Å; DLS-6 Rvalue = 0.6%)

atom	x	y	z
Si1	0.755	0.379	0.000
Si2	0.282	0.100	0.204
Si3	0.393	0.041	0.316
Si4	0.895	0.311	0.000
Si5	0.373	0.222	0.201
Si6	0.404	0.156	0.306
Si7	0.792	0.437	0.500
Si8	0.888	0.359	0.500
Si9	0.613	0.325	0.000
Si10	0.160	0.203	0.202
Si11	0.107	0.128	0.297
Si12	0.606	0.400	0.500
O1	0.275	0.098	0.092
O2	0.820	0.344	0.000
O3	0.344	0.067	0.240
O4	0.333	0.137	0.234
O5	0.393	0.000	0.723
O6	0.329	0.042	0.409
O7	0.000	0.328	0.000
O8	0.384	0.213	0.092
O9	0.265	0.215	0.230
O10	0.435	0.194	0.263
O11	0.000	0.366	0.683
O12	0.000	0.364	0.500
O13	0.839	0.398	0.500
O14	0.357	0.162	0.407
O15	0.404	0.262	0.223
O16	0.000	0.448	0.664
O17	0.647	0.366	0.000
O18	0.178	0.100	0.247
O19	0.000	0.822	0.000
O20	0.155	0.194	0.092
O21	0.129	0.169	0.263
O22	0.000	0.882	0.728
O23	0.000	0.915	0.500
O24	0.680	0.433	0.500
O25	0.122	0.125	0.408

coordinates obtained by the DLS-76 optimization of Centre. Atomic coordinates or temperature factors were not varied. To account for the intergrowth, the preferred orientation option using the stacking disorder model was applied in accordance with the observed features in the TEM study. Surprisingly, a very good fit of the experimental data was obtained, supporting the proposed model structures (Figure 8).

Most crystals in the TEM images will not have a perfect 010 orientation. Nevertheless, many images closely resemble image simulations for the new phases (Figure 9) Sometimes the specific imaging code of one of the structures can directly be recognized, e.g., Centre in Figure 5b. Therefore, the TEM information available so far is consistent with the proposed structure for COK-5. Higher resolution TEM images will be required to really confirm the structure.

Discussion and Conclusions

Planar faulting in layered materials can account for the observation of sharp and broadened reflections in diffraction patterns. Identification of the layers is necessary to model their arrangement and possible faulting to simulate corresponding diffraction patterns.

SEM and TEM analysis both prove the presence of one single phase. The flaky morphology and high-resolution TEM images have given direct evidence of a disordered layered structure. Typically, a single flake consists of 2−3 coherent zones with different crystal structure in each layer. Layers can bend or split away. TEM shows that the layers do have common structure elements, e.g., a 1.4 × 1.9 nm cell.

The channel system of MFS type zeolite is characterized by side pockets. Opposite to each other wide and small lobes are located, widening the 10 ring channels significantly. Side pockets in a straight channel system are highly appealing for catalytic purposes.[19] Bulky intermediates or transition states can be formed while only specific products can leave the reaction site through the smaller ring openings.

The described building principles for COK-5 result in two mutually independent channel systems in Mirror, Glide, and Centre. The side of the MFS layer containing the small lobes is combined into straight channels where the 10-ring aperture is opened by the narrow side pockets, giving the 10-ring channels a puckered appearance.

In the Mirror and Glide structure two types of 10-rings alternate along the channel axis with apertures of 5.6 × 6.8 and 6.7 × 4.7 Å for Mirror and 5.0 × 5.5 and 5.4 × 5.7 Å for Glide, respectively.

The lateral displacement of the Centre structure results in arrangements of identical 10-rings (6.1 × 6.2 Å) alternating in height.

The sides of the MFS layers with the wide lobes are connected to each other with the previously described click-contacts. This forms very open galleries consisting of

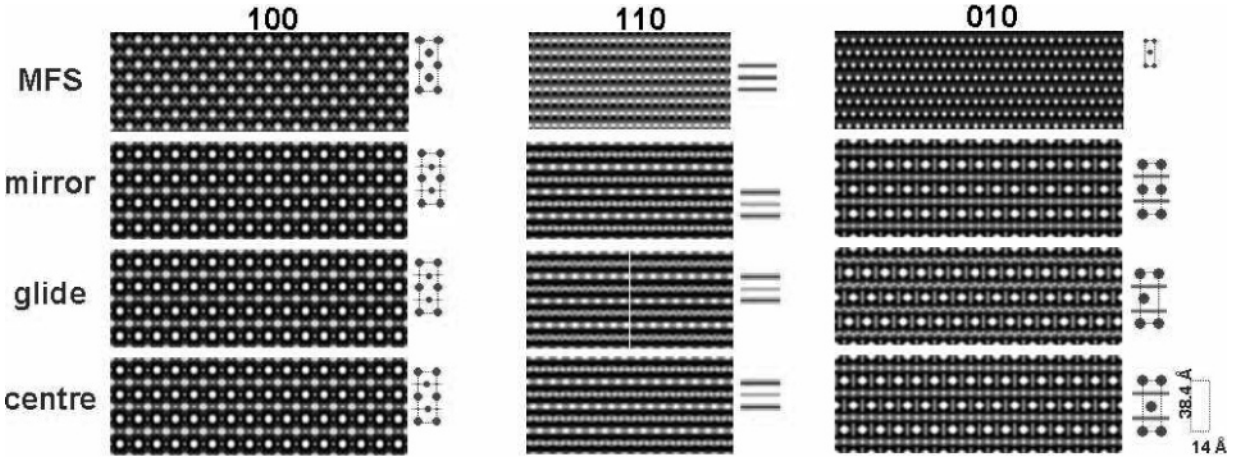

Figure 9. High-resolution TEM image simulations (MaeTempas simulation package) and imaging codes derived from them.

crossing 10- and 12-ring channels with openings of 5.5 × 4.7 and 7.5 × 4.6 Å, respectively. The galleries are identical for the three proposed structures. The wide side pockets face each other, which widens the galleries significantly to 10.5 Å at the channel crossing and to 10.8 Å along the 10-ring channels. Comparison to the 10-ring channels of ZSM-57 (5.1 × 5.4 Å) and the constrained 12-ring channels of ZSM-12 (5.6 × 6.0 Å) immediately demonstrates why the constraint index of COK-5 falls between those two materials. Even though 12-rings are present in COK-5, they are so strongly distorted that the shortest distance between oxygen atoms resembles more the distances in 10-rings than in 12-rings. This restriction, however, is more than compensated by the substantial widening along the channel axis and by the crossing of the 10-ring channels. Therefore, the pore system of COK-5 is less constrained than that in ZSM-57 where 10-rings are crossed by 8-rings. Up to now only few other topologies are known to have communicating 10- and 12-ring channels and none of the known silica topologies display such strongly distorted 12-rings which make COK-5 unique in its shape selective properties.

Acknowledgment. This work was supported by the Belgian government through the IAP-PAI network. C.E.A.K. acknowledges the Flemish FWO for a postdoctoral fellowship.

CM050227Z